Quasi-Monte Carlo, Monte Carlo, and regularized gradient optimization methods for source characterization of atmospheric releases

B Addepalli[1,4], C Sikorski[2], E R Pardyjak[1] and M Zhdanov[3]

[1] Department of Mechanical Engineering, University of Utah, Salt Lake City, UT 84112, USA
[2] School of Computing, University of Utah, Salt Lake City, UT 84112, USA
[3] Department of Geology and Geophysics, University of Utah, Salt Lake City, UT 84112, USA

Abstract. An inversion technique comprising stochastic search and regularized gradient optimization was developed to solve the atmospheric source characterization problem. The inverse problem comprises retrieving the spatial coordinates, source strength, and the wind speed and wind direction at the source, given certain receptor locations and concentration values at these receptor locations. The Gaussian plume model was adopted as the forward model and derivative–based optimization was preferred to take advantage of its simple analytical nature. A new misfit functional that improves the inversion accuracy of atmospheric inverse-source problems was developed and used in the solution procedure. Stochastic search was performed over the model parameter space to identify a good initial iterate for the gradient scheme. Several Quasi-Monte Carlo point-sets were considered in the stochastic search stage and their best performance is shown to be 5 to 100 times better than the Mersenne-Twister pseudorandom generator. Newton's method with the Tikhonov stabilizer and adaptive regularization with quadratic line-search was implemented for gradient optimization. As the forward modelling and measurement errors for atmospheric inverse problems are usually unknown, issues concerning 'model-fit' and 'data-fit' were examined. In this paper, the workings and validation of the proposed approach are presented using field experiment data.

Introduction

The solution of inverse problems involves the retrieval of information about a physical process or phenomenon from known or observed data [48]. Inverse problems arise in various fields and hence techniques to solve such problems have been an area of extensive study. One of the contemporary applications of inversion techniques includes the source characterization problem for atmospheric contaminant dispersion. Atmospheric source characterization problems, also referred to as event reconstruction, source-inversion or inverse-source problems, comprise characterizing the source of a chemical / biological / radiological (CBR) agent released into the atmosphere. Source characterization typically involves predicting the release location and rate of the CBR agent and the meteorological conditions at the release site, based on the time-averaged concentration and wind measurements obtained from a distributed sensor network in the region of interest. In this paper, an inversion technique developed to retrieve the spatial coordinates, source strength, and the wind speed and wind

[4]Corresponding author: Bhagirath Addepalli, Department of Mechanical Engineering, MEB 2110, University of Utah, Salt Lake City, UT - 84112, U.S.A.

Dagstuhl Seminar Proceedings 09391
Algorithms and Complexity for Continuous Problems
http://drops.dagstuhl.de/opus/volltexte/2009/2299

direction at the source, using concentration values from known receptor locations in the domain is described.

Efficient and robust event reconstruction tools can play a crucial role in the event of accidental or deliberate release of CBR agents in or close to urban centres. Under such circumstances, quick and accurate reconstruction can help government agencies evacuate people from the affected regions. Also, using the information obtained from inversion, forward models can be run to estimate the extent of the plume spread and the consequent exposure. Event reconstruction tools can also be of use to environmental monitoring agencies as they can help evaluate the contribution of the stack releases from various industries close to urban areas to the air quality within urban areas. Therefore, from the perspective of public safety and national security, a fast, robust, and accurate atmospheric event reconstruction tool is pivotal for air-quality management and to effectively deal with emergency response scenarios.

Given that the subject of source characterization of atmospheric contaminant dispersion is in its infancy, researchers have examined the applicability and effectiveness of the various available inversion procedures to solve such problems. The solution methodologies used span the range of deterministic (adjoint methods), stochastic (simulated annealing (SA), genetic algorithms (GA), Bayesian inference using Markov Chain Monte Carlo sampling (MCMC)) and 'common-sense' methods (collector footprint methods). The inverse-source problem has been solved over local, regional and continental scales for different model parameters (m) using empirical, diagnostic and prognostic models for scalar transport as the forward operator (A). Table 1 summarizes the salient features of the inversion procedures adopted by some of the research groups across the world to solve the inverse-source problem.

In this paper, an approach that has the combined benefits of stochastic search and gradient descent methods is presented. The workings of proposed approach are explained using field experiment data (The Copenhagen Tracer Experiments – TCTE) [17]. The objective of conducting stochastic search is to provide the gradient optimization scheme a good starting solution. It should be noted that the stochastic search is not a guided-search and this ensures that the misfit functional space has been adequately sampled, thereby eliminating the possibility of getting stuck in a sub-optimal region. Three strategies for solving the inverse-source problem in general and computing the 'data-fit' criterion for the stochastic search stage in particular are discussed. Gradient optimization is performed with the initial iterate provided by the stochastic search stage until the global minimum is reached. The 'model-acceptancy' criterion for the gradient scheme was based on the difference between predicted model parameters in the iteration space. The Gaussian plume dispersion model was adopted as the forward model (A) because of its theoretical and computational simplicity.

Apart from the hybrid approach proposed, the present paper also investigated some of the vital aspects of the atmospheric source characterization problem when using the Gaussian plume model as the forward operator. The first feature examined was the effect of the misfit functional formulation on the accuracy and complexity of inversion. Based on this study, a new misfit functional that into account both the zero and non-zero measurements recorded by the receptors and improves the inversion accuracy of atmospheric inverse-source problems was developed and used in the solution procedure. Several Quasi-Monte Carlo point-sets were considered in the stochastic search stage and their best performance is shown to be 5 to 100 times better than the Mersenne-Twister pseudorandom generator. The choice of the descent methods (steepest descent, Newton's, and conjugate gradient methods), stabilizing functional (Tikhonov), and the regularization parameter for gradient optimization were also examined. Gradient descent methods are an attractive choice for the current problem as analytical expressions for the Frechet and Hessian can be pre-computed for the Gaussian plume equation. For the current inverse problem, Newton's method with adaptive regularization and quadratic line-search was implemented. Since the forward modelling and measurement errors for atmospheric

[4]Corresponding author: Bhagirath Addepalli, Department of Mechanical Engineering, MEB 2110, University of Utah, Salt Lake City, UT - 84112, U.S.A.

inverse problems are usually unknown, the issues concerning 'model-fit' and 'data-fit' are deliberated upon.

As has been the central theme of this discussion, the area of application of inversion techniques to atmospheric source characterization problems is in its nascency and various methods are being tested and their performance is being evaluated. In the work presented in this paper, a solution procedure that is different from the ones published in the literature is suggested. As with most of the other inversion techniques, the speed and accuracy of the present solution methodology depends on the noise-level in the observed data and the quality of the forward model. When properly formulated, the solution to an inverse problem can help identify the necessary physics that need to be incorporated into the forward model. Thus, inverse problems can in-turn be used to improve the speed and accuracy of the solution to the forward problem by enhancing or pruning the forward model.
Problem definition

1.1. The forward problem
The Gaussian plume model (GPM) is the simplest model that describes the dispersion of atmospheric contaminants. Accordingly, the inverse-source problem was solved using the GPM for continuous point-releases as the forward operator (A). The GPM for steady, continuous and uniform wind conditions can be written as [9, 43]:

$$C_R(x_R, y_R, z_R) = \frac{Q_S}{2 \cdot \pi \cdot u_S \cdot \sigma_y \cdot \sigma_z} e^{\frac{-y^2}{2\sigma_y^2}} \cdot \left\{ e^{\frac{-(z_R - z_S)^2}{2 \cdot \sigma_z^2}} + e^{\frac{-(z_R + z_S)^2}{2 \cdot \sigma_z^2}} \right\} \tag{2.1.1}$$

$$\sigma_y = \frac{C_1 \cdot x}{\sqrt{1 + 0.0004 \cdot x}}; \;\; \sigma_z = C_2 \cdot x \tag{2.1.2}$$

$$x = -(y_R - y_S) \cdot Cos(\theta_S) - (x_R - x_S) \cdot Sin(\theta_S) \tag{2.1.3}$$

$$y = -(y_R - y_S) \cdot Sin(\theta_S) + (x_R - x_S) \cdot Cos(\theta_S) \tag{2.1.4}$$

Equation (2.1.1) gives an estimate of the concentration at a receptor (C_R) with the position vector $\vec{X} = \left[(x_R - x_S), (y_R - y_S), (z_R - z_S)\right]$; where, x_S, y_S, z_S, and x_R, y_R, z_R, represent the source and receptor coordinates respectively. The emission rate is Q_S, and the wind speed (u_S), and direction (θ_S) are assumed to be constant over the region of interest. The distances ($x_R - x_S$), ($y_R - y_S$), and ($z_R - z_S$) are measured in the along-wind, cross-wind, and vertical directions with the origin of the coordinate system being the source location. The parameters σ_y and σ_z (equation (2.1.2)) are called the Gaussian plume spread parameters and account for the turbulent diffusion of the plume. They are empirical parameters and are defined for various meteorological stability conditions. For the present problem, Brigg's formulae for Pasquill C-type stability conditions were chosen [9, 43]. These parameters, however, are terrain and problem dependent and therefore for the present work, the empirical constants C_1 and C_2, which in Brigg's formulae are 0.22 and 0.20, were replaced by 0.12 and 0.10 for TCTE [17] as per the work of [36]. There are several other assumptions that are tacit in the Gaussian dispersion equation for which the reader may refer to [9, 43].

The forward problem can be defined as estimating the concentrations at the desired receptor locations based on the given model (source) parameters (m) and can be written as:

$$A(m) = d \tag{2.1.5}$$

[4]Corresponding author: Bhagirath Addepalli, Department of Mechanical Engineering, MEB 2110, University of Utah, Salt Lake City, UT - 84112, U.S.A.

where, A is the forward modelling operator (which in this case is the GPM), m is the set of model or source parameters, and d is the vector of concentration measurements at the various receptor locations (denoted by subscripts R1, R2….RN respectively). For the computation of the concentration values at any point downwind of the source, the GPM requires eight model parameters (m_{GPM}). Hence, when using the GPM as the forward model (A), equation (2.1.5) can be written as:

$$A(m_{GPM}) = d \tag{2.1.6}$$

$$m_{GPM} = \begin{bmatrix} x_S & y_S & z_S & Q_S & u_S & \theta_S & C_1 & C_2 \end{bmatrix}^T_{8\times1} \tag{2.1.7}$$

$$d = \begin{bmatrix} C_{R1} & C_{R2} & \bullet & \bullet & \bullet & \bullet & C_{RN} \end{bmatrix}^T_{N\times1} \tag{2.1.8}$$

1.2. The inverse problem

The inverse problem can be defined as the solution of the operator equation:

$$d = A(m) \tag{2.2.1}$$

The solution to the inverse problem requires determining a model 'm_{pr}' (predicted model) that generates predicted data, 'd_{pr}', which 'fits-well' the observed data 'd_{obs}' [48]. Since the forward operator (A) is nonlinear, the solution to the inverse problem can only be found iteratively. Therefore, nonlinear inverse problems are often cast as minimization or optimization problems as shown below:

$$\arg\left(\min_{m_{pr}} \left\| A(m_{pr}) - d_{obs} \right\|^2 \right) \tag{2.2.2}$$

From equations (2.1.1) and (2.1.7) it can be deduced that when solving the source inversion problem using the GPM, at most eight model parameters can be retrieved (m_{GPM}). Of these eight parameters, since the source strength (Q_S) and the wind velocity at the source (u_S) are a fraction of each other in the Gaussian equation (equation (2.1.1)), attempting to retrieve them individually can result in non-unique solutions for these parameters. Therefore, they were combined into a single term (Q_S / u_S) in the present solution procedure. Five ($m_{STOCH+GD}$) (equation (2.2.3)) of the eight model parameters (m_{GPM}) (equation (2.1.7)) in the GPM (Q_S and u_S combined into a single term (Q_S / u_S)) were retrieved in the present work for TCTE. Hence, the inverse-source problem is a five dimensional (5D) inverse problem.

$$m_{STOCH+GD} = \begin{bmatrix} x_S & y_S & z_S & Q_S / u_S & \theta_S \end{bmatrix}^T_{5\times1} \tag{2.2.3}$$

Validation tests – the Copenhagen tracer experiments (TCTE)

In this paper, data from TCTE [17] has been used to explain the workings, as well as to validate the proposed approach. As part of this experiment, the tracer sulphurhexafluoride (SF_6) was released without buoyancy from a tower of height 115 m. It was collected 2 – 3 m above the ground-level by sensors placed in three crosswind arcs positioned 2 – 6 km from the point of release. The first (Arc 1), second (Arc 2), and third (Arc 3) arcs were at radial distances of 2km, 4km, and 6km from the source. The receptor locations and the source release location are shown in figure 1. A total of 137 tracer-samplers were used with 48 sensors placed in Arc 1, 46 in Arc 2, and 43 in Arc 3. Three consecutive 20 minute averaged tracer concentrations were measured, allowing for a total sampling time of 1 hour. The site was mainly residential having a roughness length (z_0) of 0.6 m. The experiment was conducted on different days under neutral and unstable meteorological stability conditions. For the present work, the experiment conducted on October 19, 1978 / 1979 was considered. The meteorological stability class was Pasquill C–type, emission rate was 3.2 g / s, and the limit of

[4]Corresponding author: Bhagirath Addepalli, Department of Mechanical Engineering, MEB 2110, University of Utah, Salt Lake City, UT - 84112, U.S.A.

estimation (LOE) of the sensors was 9 ng / m^3. The wind speed (u_S) and direction (θ_S) at the release height during the course of the experiment were $u_S \sim 4.92$ m / s and $\theta_S \sim 308.57$ degrees. For the validation of the proposed inversion technique, the height of the sensors was considered to be 2.5 m.

It is worth noting that for the October 19 experiment, 34 out of the 137 sensors received a hit. These have been denoted by the 'squares' (□) in figure 1. As stated in the introductory section, the total error that needs to be accounted for during the estimation stage is the sum of the following individual error components:

$$\text{Estimation error } (\delta_E) = \text{forward modelling error } (\delta_{FM}) + \text{measurement error } (\delta_M) \qquad (3.1)$$

Since the authors of the report make no mention of the uncertainties in the measurements, δ_M was assumed to be zero (i.e., $\delta_E = \delta_{FM}$). In order to get a feel for δ_{FM} when using the GPM, the forward problem was solved with the known source parameters, with $C_1 \sim 0.12$ and $C_2 \sim 0.10$ (from the work of [36]). The results obtained are shown in figure 1. From the figure it is evident that despite using the modified σ_y and σ_z values, the plume spread predicted by the GPM does not match the experimental measurements.

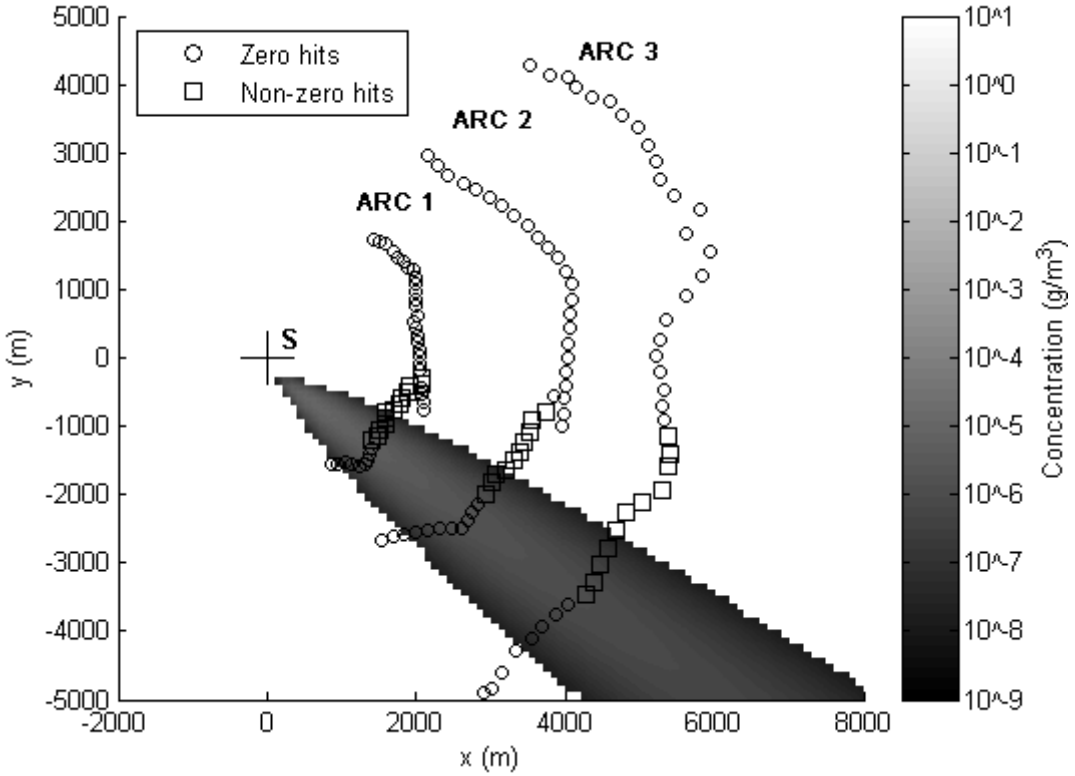

Figure 1: Schematic depicting the sensor positioning and the number of zero (o) and non-zero (□) measurements recorded for TCTE on October 19. Also shown is the plume spread predicted by the GPM for true source parameters (m_t). 'S' is the true source location.

The difference in the plume spread predicted by the GPM can be attributed to the complexities associated with real-world flows that have not been incorporated into the present version of the GPM. Since $\delta_E = \delta_{FM}$, and δ_{FM} is due to the inadequacies of the forward model (A) and cannot be quantified, the inversion procedure developed (and described in subsequent sections) was designed to drive the forward model (A) to match the zero and non-zero measurements recorded by the sensors. That is, the

[4]Corresponding author: Bhagirath Addepalli, Department of Mechanical Engineering, MEB 2110, University of Utah, Salt Lake City, UT - 84112, U.S.A.

inversion procedure developed ensures that at the end of inversion, the plume spread predicted by the GPM is as close as possible to that observed in the experiments, not in terms of magnitudes of concentration measurements, but, in terms of the zero and non-zero measurements recorded by the respective sensors. Whenever the predicted model parameters generate non-zero (≥ LOE) predicted data at a receptor that recorded a non-zero concentration (≥ LOE), or zero (< LOE) predicted data at a receptor that recorded a zero concentration value (< LOE), it will from hereon be said that the predicted model parameters 'satisfy' the concentration measurement at the receptor location.

The true model parameters (m_t) for TCTE that were retrieved using the proposed approach are shown in equation (3.2). The bounds of the model parameter space considered during inversion are shown in equation (3.3).

$$m_t = \begin{bmatrix} x_S & y_S & z_S & Q_S/u_S & \theta_S \end{bmatrix}^T_{5\times1} = \begin{bmatrix} 0 & 0 & 115 & 0.65 & 308.57° \end{bmatrix}^T_{5\times1} \tag{3.2}$$

$$x_S \in [-2000,8000] \quad y_S \in [-5000,5000] \quad z_S \in [0,200] \quad Q_S/u_S \in [0,1] \quad \theta_S \in [0,360] \tag{3.3}$$

Solution procedure

1.3. The Tikhonov parametric functional

In a general setting, the solution to an inverse problem can be obtained by minimizing the following unconstrained parametric functional [48]:

$$P^{\alpha}(m_{\alpha}, d_{\delta}) = \mu_D^2(A(m_{\alpha}), d_{\delta}) + \alpha \cdot s(m_{\alpha}) \tag{4.1.1}$$

$$\arg\left(\min_{m_{\alpha}} \left(P^{\alpha}(m_{\alpha}, d_{\delta}) \right) \right) \tag{4.1.2}$$

This can also be written as:

$$p(\alpha) = i(\alpha) + \alpha \cdot s(\alpha) \tag{4.1.3}$$

where $i(\alpha) = \mu_D^2(A(m_{\alpha}), d_{\delta})$ is the misfit functional, $s(\alpha) = s(m_{\alpha})$ is the stabilizing functional, and $p(\alpha) = P^{\alpha}(m_{\alpha}, d_{\delta})$ is the parametric functional. The parametric functional $p(\alpha)$ is a linear combination of the misfit and the stabilizing functionals, and the unknown real parameter α is called the regularization parameter.

The parametric functional described in equation (4.1.1) can be minimized using different techniques. Depending upon the technique chosen, the inversion procedure acquires its respective name (such as GA, SA, gradient descent, adjoint methods, etc.). In this paper, equation (4.1.1) was minimized using gradient descent methods.

1.4. The misfit functional

Since atmospheric inverse–source problems suffer from sparse number of measurements (N) in general, and, very few non-zero measurements (N_{NZ}) in particular, a new misfit functional that takes into account the non-zero measurements was developed and was used in the stochastic stage. It is based on the ideas of log-likelihood and is shown through equations (4.2.5) to (4.2.10) below (Formulation). The constant ε ($\varepsilon << LOE$) accounts for the zero hits and becomes insignificant for non–zero hits. For the present work, ε value was set to 10^{-16}.

[4]Corresponding author: Bhagirath Addepalli, Department of Mechanical Engineering, MEB 2110, University of Utah, Salt Lake City, UT - 84112, U.S.A.

Formulation of the new misfit functional:

$$d_{obs} = \left[C_{R1} \quad C_{R2} \quad . \quad . \quad . \quad . \quad C_{RN} \right]^{T}_{N\times 1} \tag{4.2.5}$$

$$d_{pr} = \left[\left(A(m_{pr})\right)_{R1} \quad \left(A(m_{pr})\right)_{R2} \quad . \quad . \quad . \quad . \quad \left(A(m_{pr})\right)_{RN} \right]^{T}_{N\times 1} \tag{4.2.6}$$

$$D_{\varepsilon} = \left[\log_{10}\left(\frac{d_{obs_{R1}} + \varepsilon}{d_{pr_{R1}} + \varepsilon} \right) \quad \log_{10}\left(\frac{d_{obs_{R2}} + \varepsilon}{d_{pr_{R2}} + \varepsilon} \right) \quad . \quad . \quad . \quad \log_{10}\left(\frac{d_{obs_{RN}} + \varepsilon}{d_{pr_{RN}} + \varepsilon} \right) \right]^{T}_{N\times 1} \tag{4.2.7}$$

$$Define: D^{+}_{\varepsilon}(i) = \begin{cases} D_{\varepsilon,i} & if\ D_{\varepsilon,i} \geq 0 \\ 0 & otherwise \end{cases}$$

$$Define: D^{-}_{\varepsilon}(i) = \begin{cases} D_{\varepsilon,i} & if\ D_{\varepsilon,i} < 0 \\ 0 & otherwise \end{cases} \tag{4.2.8}$$

$$such\ that\ D^{+}_{\varepsilon} + D^{-}_{\varepsilon} = D_{\varepsilon}$$

$$Compute: \kappa_{LB} = -\left\| D^{-}_{\varepsilon} \right\|_{\infty}\ and\ \kappa_{UB} = \left\| D^{+}_{\varepsilon} \right\|_{\infty} \tag{4.2.9}$$

$$Solve\ until:\ \kappa_{LB} \geq \beta_{LB-STOCH}\ and\ \kappa_{UB} \leq \beta_{UB-STOCH} \tag{4.2.10}$$

The new misfit functional was used in the stochastic search stage to identify a good starting solution for the gradient descent scheme. Since gradient methods only work for convex misfit functionals, the conventional misfit functional based on L_2–norm was used for computing the new iterates for the gradient scheme.

1.5. Strategies for solving the atmospheric source inversion problem

In this section, strategies for solving the atmospheric source characterization problem in general and computing the bounds $\beta_{LB-STOCH}$ and $\beta_{UB-STOCH}$ in particular are discussed. Three strategies are proposed to solve the inverse-source problem. They are described in the following sections:

4.3.1. Rigorous strategy: The objective of this strategy is to 'satisfy' (defined in section 3) all the sensor measurements (N), if not in magnitude, then at least in terms of the number of zero (N_Z) and non-zero (N_{NZ}) measurements. In spite of being the most rigorous method to solve such problems, this approach cannot be implemented for all real-life atmospheric dispersion situations and for increasing number of sensor measurements (N). This is because, the effects of myriads of real-world processes are not captured in totality by the existing forward dispersion models (A) in general, and the GPM in particular.

4.3.2. Semi-rigorous strategy: The objective of this strategy is to satisfy most, but not all the sensor measurements (N). The number of sensor measurements that should be satisfied (N_S), or the percentage of the total number of measurements (N) that should be satisfied (λ_N=100×N_S / N) for the predicted solution to be in the vicinity of the true solution is problem-specific, and depends upon the number of available sensor measurements (N), the number of model parameters to be retrieved (N_m), and the quality of the forward model (A). While λ_N values close to 100% make the stochastic search stage computationally intensive, relaxed values of λ_N might produce initial iterates that do not belong to the C-C-D region surrounding the global minimum.

It should be noted that while solving inverse-source problems, fixing values of N_S might result in erroneous source locations. This is because the inversion algorithm might end up not accounting for either only the zero or non-zero measurements to satisfy the λ_N value assigned. To avoid such pitfalls,

[4]Corresponding author: Bhagirath Addepalli, Department of Mechanical Engineering, MEB 2110, University of Utah, Salt Lake City, UT - 84112, U.S.A.

it is suggested that N_S should be divided into its individual components that are based on the number of zero ($N_{S\text{-}Z}$) and non-zero ($N_{S\text{-}NZ}$) measurements ($N_S = N_{S\text{-}Z} + N_{S\text{-}NZ}$). Assigning λ_N values based on the percentage of zero ($\lambda_Z = 100 \times N_{S\text{-}Z} / N_Z$) and non-zero ($\lambda_{NZ} = 100 \times N_{S\text{-}NZ} / N_{NZ}$) measurements will improve the accuracy of the inversion algorithm. Based on how the λ_N values are determined, the semi-rigorous strategy can be implemented in three ways. They are:

4.3.2.1 Semi-rigorous strategy 1 (SR1): SR1 comprises satisfying λ_N measurements without assigning individual values for λ_{NZ} and λ_Z. To evaluate the performance of the various QMC point-sets, the number of MC and QMC points required for satisfying N_S = 128, 129, and 130 sensors are compared in this paper.

4.3.2.2 Semi-rigorous strategy 2 (SR2): SR2 comprises assigning individual values for λ_{NZ} and λ_Z. In this paper results for the cases starting from $\lambda_{NZ} = \lambda_Z = 90\%$ and in increments of 1% until $\lambda_{NZ} = \lambda_Z = 95\%$ are discussed.

4.3.2.3 Semi-rigorous strategy 3 (SR3): In SR3, λ_{NZ} value is always set at 100% and $\lambda_Z \in [90\%, 100\%]$. For evaluating the performance of the various QMC point-sets, results for the cases when $\lambda_Z = [90\%, 91\%, 92\%, 93\%]$ are reported. The expected number of MC simulations (E(MC)) required for SR1, SR2, and SR3 are shown in figure 2.

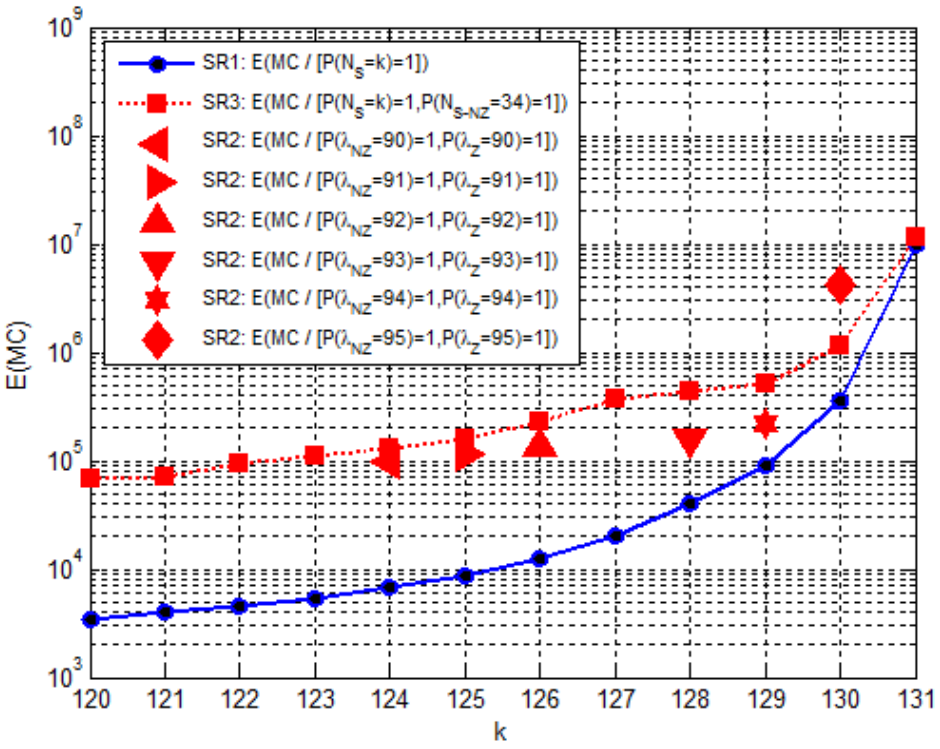

Figure 2: Expected number of MC simulations (E(MC)) for SR1, SR2, and SR3

1.6. Computing the bounds $\beta_{LB-STOCH}$ *and* $\beta_{UB-STOCH}$

[4]Corresponding author: Bhagirath Addepalli, Department of Mechanical Engineering, MEB 2110, University of Utah, Salt Lake City, UT - 84112, U.S.A.

The bounds $\beta_{LB-STOCH}$ and $\beta_{UB-STOCH}$ can be derived through the understanding of the GPM and atmospheric contaminant dispersion. For atmospheric flows, the bounds $\beta_{LB-STOCH}$ and $\beta_{UB-STOCH}$ may be estimated as:

$$\beta_{LB-STOCH} \approx \log_{10}\left[\frac{\varepsilon}{LOE}\right] \approx \log_{10}\left[\frac{10^{-16}}{9\cdot 10^{-9}}\right] \approx -7.95 \tag{4.5.1}$$

$$\beta_{UB-STOCH} \approx \log_{10}\left[\frac{LOE}{\varepsilon}\right] \approx \log_{10}\left[\frac{9\cdot 10^{-9}}{10^{-16}}\right] \approx 7.95 \tag{4.5.2}$$

1.7. MC and QMC sampling

QMC point-sets and MC sampling were considered in the stochastic search stage. QMC sampling was performed using the Halton, Hammersley, Sobol, SpecialNeiderreiter, and NeiderreiterXing point-sets, in their original and scrambled forms. The scrambled versions of the Halton, Hammersley, SpecialNeiderreiter, and NeiderreiterXing point-sets were obtained by applying Faure permutations over the original set [15]. The scrambled version of the Sobol point-set was obtained by applying the MatousekAffineOwen scrambling procedure [30], a random linear scramble combined with a random digital shift.

1.8. The stabilizing functional, regularization parameter, and gradient methods

For the inverse-source problem, the standard Tikhonov stabilizing functional was chosen as the penalty functional. The Tikhonov stabilizer is shown in equation (4.6.1) below. m_{apr} represents some prior information that we might have about the model parameters (m). No prior information was assumed in the solution procedure for the atmospheric event reconstruction problem. However, a modified version of the stabilizer shown in equation (4.6.1) was used in the descent algorithms and is shown in equation (4.6.2).

$$s(m) = \left\| m - m_{apr} \right\|_2^2 \tag{4.6.1}$$

$$s(m) = \left\| m_i - m_{i-1} \right\|_2^2; i = 2,3..... \tag{4.6.2}$$

The regularization parameter α determines the relative significance of the misfit and the stabilizing functionals. In the present paper, a heuristic approach to determine α as suggested in [48] was adopted. The regularization parameter was estimated following equations (4.6.3) and (4.6.4) shown below.

$$\alpha_1 = \frac{\left\| A(m_1) - d_{obs} \right\|_2^2}{\left\| m_1 - m_0 \right\|_2^2} \tag{4.6.3}$$

$$\alpha_i = \alpha_1 \cdot q^{i-1};\ (0 < q < 1);\ i = 2,3,..... \tag{4.6.4}$$

Following equations (4.2.2), (4.6.2), (4.6.3) and (4.6.4), the unconstrained parametric functional described in equation (4.1.1) can be written as:

$$P_i^{\alpha}(m_{\alpha}, d_{\delta}) = \left\| A(m_i) - d_{obs} \right\|_2^2 + \alpha_i \cdot \left\| m_i - m_{i-1} \right\|_2^2 \tag{4.6.5}$$

[4]Corresponding author: Bhagirath Addepalli, Department of Mechanical Engineering, MEB 2110, University of Utah, Salt Lake City, UT - 84112, U.S.A.

The parametric functional shown in equation (4.6.5) was minimized using Newton's method. To ensure convergence and to prevent overshooting of the Newton jump, quadratic line-search was implemented. Additional details of the algorithm implemented can be found in [48].

Results and Discussion

The results obtained by implementing the solution procedure described in section 4 are presented in this section.

1.9. Need for considering both zero and non-zero measurements

As stated in the introductory section and section 4.2, the accuracy of inversion improves when both zero and non-zero measurements are considered. To illustrate this fact, model parameters for TCTE were retrieved by considering, a) only the non-zero measurements, and b) both zero and non-zero measurements. The rigorous strategy was used when only the non-zero measurements were considered (N_{NZ} = 34). SR1 with N_S = 128 was used when both zero and non-zero measurements were considered. For these simulations, the Mersenne-Twister generator was used in the stochastic search stage. The results obtained are shown in Table 2.

'm_t' represents the true model parameters from TCTE. '$m_{(STOCH)*(NZ)}$' and '$m_{(STOCH+GD)*(NZ)}$' stand for the initial iterates and the final model parameters provided by the stochastic stage and Newton's method when only non-zero measurements were considered. '$m_{(STOCH)*(Z+NZ)}$' and '$m_{(STOCH+GD)*(Z+NZ)*avg}$' represent the initial iterates and the final model parameters provided by the stochastic stage and Newton's method when both zero and non-zero measurements were considered. In the present work, convergence of the Newton's method is determined based on both the L_2 - norm of the residual as well as N_S values in the iteration space. This is illustrated in figure 5, where convergence of Newton's method is shown for cases when only zero (figure 5(a)) and both zero and non-zero measurements (figure 5(b)) were considered. When only non-zero measurements were considered, since the stochastic stage was implemented with the rigorous strategy, the N_S value in the iteration space of Newton's method is constant (N_S = 34; N_{NZ} = 34) (figure 5(a)). However, when both zero and non-zero measurements are considered, since N = 137, and N_S = 128, Newton's method can generate model parameters with N_S values above and below 128 before reaching the global minimum. Based on the values of $\left\| A(m_{pr}) - d_{obs} \right\|_2$ in the iteration space, as well several '$m_{(STOCH)*(Z+NZ)}$' (using the Mersenne-Twister generator), it was found that when the Newton's method converged, it converged at N_S = 129, after about 70 iterations (figure 5(b)) when SR1 was employed. Therefore in Table. 2, model parameters that satisfy N_S = 129 and result in the minimum residual, as well as model parameters corresponding to the maximum N_S value ($m_{(STOCH+GD)*(Z+NZ)*max(Ns)}$) are presented.

From the results in Table. 2 it can be seen that inversion accuracy improves when both zero and non-zero measurements are considered. That is, '$m_{(STOCH+GD)*(Z+NZ)\ *avg}$' is closer to '$m_t$' when compared to '$m_{(STOCH+GD)*(NZ)}$'. Also, it is seen that '$m_{(STOCH+GD)*(Z+NZ)\ *avg}$' and '$m_{(STOCH+GD)*(Z+NZ)*max(Ns)}$' are closer to '$m_t$' in different components.

Irrespective of the strategy (SR1, SR2, and SR3) chosen to identify an initial iterate, Newton's method always converged to the final model parameters given by '$m_{(STOCH+GD)*(Z+NZ)\ *avg}$'. Therefore, only the performance of the various QMC point-sets in terms of number of points required for identifying an initial iterate are discussed in the subsequent sections (section 5.2). The performance of the Newton's method in terms of number of iterations required to converge to the final solution depending on the strategy chosen is discussed in section 5.3.

Table 2: Inversion results comparison considering non-zero versus zero + non-zero measurements

[4]Corresponding author: Bhagirath Addepalli, Department of Mechanical Engineering, MEB 2110, University of Utah, Salt Lake City, UT - 84112, U.S.A.

Model parameters	x_S (m)	y_S (m)	z_S (m)	q_S / u_S (g / m)	θ_S (degrees)	N_S
m_t	0	0	115	0.64	308.57	----
$m_{(STOCH)*(NZ)}$	-1785.68	495.14	190.47	0.69	292.30	34
$m_{(STOCH+GD)*(NZ)}$	-340.39	73.87	193.43	1.07	291.73	34
$m_{(STOCH)*(Z+NZ)}$	667.60	-697.63	102.97	0.45	287.17	128
$m_{(STOCH+GD)*(Z+NZ)*avg}$	-94.64	-15.38	163.12	0.78	293.13	129
$m_{(STOCH+GD)*(Z+NZ)*max(Ns)}$	-7.15	-130.36	178.00	0.78	291.50	130

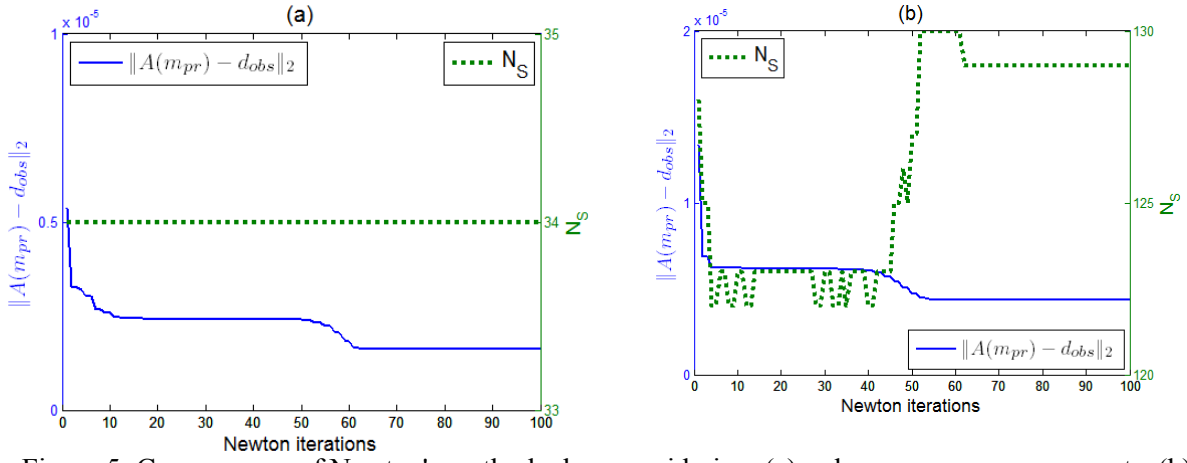

Figure 5: Convergence of Newton's method when considering, (a) only non-zero measurements, (b) both zero and non-zero measurements

1.10. Performance of the various QMC point-sets in the stochastic search stage

The performance of the various QMC point-sets for SR1, SR2, and SR3 for the different λ values described in sections 4.3.2.1 (SR1), 4.3.2.2 (SR2), and 4.3.2.3 (SR3) is compared against the Mersenne-Twister pseudorandom generator. The expected value of the number of random samples required (E(MC)) for these cases can be found in figure 5. In the stochastic search stage, the number of QMC points required to satisfy a given λ value (λ = k) was determined by the number of points that satisfy λ ≥ k. The results obtained are reported in Tables 3 to 8.

In Tables 3 to 8, MC stands the expected number of random samples (E(MC)) required from the Mersenne-Twister generator to satisfy the given criteria. The letters 'O' and 'S' before the various QMC point-sets are indicative of their original or scrambled nature. 'SplNie' and 'NieXing' are abbreviations for the SpecialNiederreiter and Niederreiter point-sets.

Based on the results obtained for SR1, SR2, and SR3 from Tables 3 to 8 the following can be concluded: 1) The QMC point-sets on an average perform better then Mersenne-Twister generator for most of the cases. 2) Of all the QMC point-sets, the Halton point-set (original and scrambled), and the original Sobol sequence perform better than the others (and the Mersenne-Twister generator).

The arguments based on which the Halton (original and scrambled) and the original Sobol point-sets were determined to be the best of the point-sets considered are as follows: 1) The Hammersley point-set is not recommended as its first dimension is the regular one-dimensional lattice evenly distributed on the interval [0, 1). Therefore, based on the number of points generated, the Hammersley sequence changes in the first dimension. Since the optimum number of points that should be generated for identifying the initial iterate with the fewest possible points is not known apriori, the Hammersley point-set is not recommended. Also, if the proposed approach is implemented with initial λ = 90%

[4]Corresponding author: Bhagirath Addepalli, Department of Mechanical Engineering, MEB 2110, University of Utah, Salt Lake City, UT - 84112, U.S.A.

option, and if the λ value needs to be incremented subsequently, the entire simulation should be re-run if the Hammersley sequence is used. For the purposes of comparison against the Mersenne-Twister generator, in the present paper, the number of Hammersley points generated for a given strategy and λ value was set equal to E(MC) for that strategy and λ value. 2) Apart from the Halton and original Sobol point-sets, all other point-sets exceed the number of MC points required in at least one of the reported results in Tables 3 to 8. Such results are indicated by either the asterisk superscript (*), or have not been reported (indicated by ----------) (whenever the number of QMC points required is much larger than E(MC)).

Table 3: Performance of the various original QMC point-sets with SR1

Point-sets	$N_S = 128$	$N_S = 129$	$N_S = 130$
MC	40,656	92,075	350,789
O-Halton	3,749	54,581	237,389
O-Hammersley	8,322	----------	----------
O-Sobol	31,645	47,213	47,213
O-SplNie	87,016****	108,377****	398,025****
O-NieXing	49,906****	70,527	159,266

Table 4: Performance of the various scrambled QMC point-sets with SR1

Point-sets	$N_S = 128$	$N_S = 129$	$N_S = 130$
MC	40,656	92,075	350,789
S-Halton	797	43,565	198,437
S-Hammersley	4,546	17,314	64,767
S-Sobol	3,474	119,338****	359,538****
S-SplNie	1,897	1,897	28,248
S-NieXing	11,371	21,339	21,339

Table 5: Performance of the various original QMC point-sets with SR2

Point-sets	$\lambda_{NZ} = \lambda_Z = 90\%$	$\lambda_{NZ} = \lambda_Z = 91\%$	$\lambda_{NZ} = \lambda_Z = 92\%$	$\lambda_{NZ} = \lambda_Z = 93\%$	$\lambda_{NZ} = \lambda_Z = 94\%$	$\lambda_{NZ} = \lambda_Z = 95\%$
MC	*96,658*	*116,327*	*133,473*	*157,889*	*223,821*	*4,166,667*
O-Halton	3,749	3,749	9,293	9,293	64,733	1,659,029
O-Hammersley	16,162	14,986	16,946	30,463	46,143	886,402
O-Sobol	877	877	31,645	47,213	146,445	918,285
O-SplNie	10,672	22,993	22,993	108,377	108,377	----------
O-NieXing	10,633	10,633	49,906	70,527	70,527	4,660,113****

Table 6: Performance of the various scrambled QMC point-sets with SR2

Point-sets	$\lambda_{NZ} = \lambda_Z = 90\%$	$\lambda_{NZ} = \lambda_Z = 91\%$	$\lambda_{NZ} = \lambda_Z = 92\%$	$\lambda_{NZ} = \lambda_Z = 93\%$	$\lambda_{NZ} = \lambda_Z = 94\%$	$\lambda_{NZ} = \lambda_Z = 95\%$
MC	*96,658*	*116,327*	*133,473*	*157,889*	*223,821*	*4,166,667*
S-Halton	797	797	797	43,565	43,565	198,437
S-Hammersley	13,394	13,394	25,567	33,407	5,4015	887,554
S-Sobol	3,474	3,474	3,474	3,474	199,778	1,205,466

[4]Corresponding author: Bhagirath Addepalli, Department of Mechanical Engineering, MEB 2110, University of Utah, Salt Lake City, UT - 84112, U.S.A.

S-SplNie	3,385	15,505	15,505	15,505	106,825	----------
S-NieXing	6,087	6,087	6,087	43,840	274,048****	3,314,735

Table 7: Performance of the various original QMC point-sets with SR3

Point-sets (λ_{NZ} = 100%)	λ_Z = 90%	λ_Z = 91%	λ_Z = 92%	λ_Z = 93%
MC	371,156	439,147	503,778	1,160,862
O-Halton	3,749	3,749	430,637	430,637
O-Hammersley	73,730	96,319	82,018	224,895
O-Sobol	47,213	47,213	47,213	47,213
O-SplNie	105,512	105,512	398,025	398,025
O-NieXing	17,314	159,266	159,266	159,266

Table 8: Performance of the various scrambled QMC point-sets with SR3

Point-sets (λ_{NZ} = 100%)	λ_Z = 90%	λ_Z = 91%	λ_Z = 92%	λ_Z = 93%
MC	371,156	439,147	503,778	1,160,862
S-Halton	41,621	84,389	371,885	371,885
S-Hammersley	33,554	60,994	86,082	----------
S-Sobol	119,338	119,338	119,338	712,914
S-SplNie	46,769	533,993****	827,816****	2,113,960****
S-NieXing	18,618	46,810	208,390	577,766

1.11. Overall performance of the proposed approach

The overall computational cost and thereby the execution time of the proposed approach can be divided between the stochastic and gradient stages. Depending on the strategy and the QMC point-set chosen in the stochastic stage, the computational costs and the execution times of the stochastic and the gradient stages vary. For TCTE, Newton's method took less than 100, 50, and 25 iterations when SR1, SR2, and SR3 were employed. The choice of SR1, SR2, and SR3 depends on the complexity of the problem at hand and on how much one is willing to expend on the stochastic search stage. In the present Newton's implementation, since the analytical expressions for the Frechet are pre-computed, and since the Hessian is approximated and its size is small (5×5), the main contribution to the overall computational cost and execution time comes from the stochastic stage. To get an estimate for the execution time of the present approach, stochastic search was performed using 10^5 random samples from the Mersenne-Twister generator with the required if and break statements, and 100 Newton iterations were run using the initial iterate provided by the stochastic stage. The algorithm was coded in 32-bit Matlab 7.8.0 (R2009a) and was executed on a 64-bit Dell desktop machine running Windows Vista, with 8Gb RAM, and 3.0GHz QuadCore processor. The overall execution time was ~ 38 s, with the stochastic stage taking ~ 31.5 s, and the Newton's method taking ~ 6.5s. And to reiterate, the final model parameters obtained from Newton's method were:

$$x_S \in [-2000,8000] \quad y_S \in [-5000,5000] \quad z_S \in [0,200] \qquad Q_S/u_S \in [0,1] \qquad \theta_S \in [0,360]$$

$$m_t = \left[x_S \quad y_S \quad z_S \quad Q_S/u_S \quad \theta_S\right]^T_{5\times 1} = \left[0 \quad 0 \quad 115 \quad 0.65 \quad 308.57^\circ\right]^T_{5\times 1}$$

$$m_{(STOCH+GD)*(Z+NZ)*avg} = \left[-94.64 \quad -15.38 \quad 163.12 \quad 0.78 \quad 293.13^\circ\right]^T_{5\times 1}$$

Conclusions

[4]Corresponding author: Bhagirath Addepalli, Department of Mechanical Engineering, MEB 2110, University of Utah, Salt Lake City, UT - 84112, U.S.A.

An inversion technique comprising stochastic search and regularized gradient optimization to solve the atmospheric inverse-source problem is described in this paper. The inverse problem involves retrieving the spatial coordinates, source strength, and the wind speed and wind direction at the source, given certain receptor locations and concentration values at these receptor locations. The Gaussian plume model was adopted as the forward model and derivative-based optimization was preferred to take advantage of its simple analytical nature. The workings of the proposed approach are explained using the Copenhagen field experiment data. Stochastic search is performed over the misfit functional space to identify an initial iterate for the gradient scheme. A new misfit functional was developed to take into account the zero and non-zero measurements recorded by the receptors and was used in the stochastic stage. It is based on the base 10 logarithm of the ratio of the observed and predicted data and it is shown that the new misfit functional improves the inversion accuracy. Several Quasi-Monte Carlo point-sets were considered in the stochastic search stage and their best performance is shown to be 5 to 100 times better than the Mersenne-Twister pseudorandom generator. QMC point-sets are recommended for atmospheric inverse-source problems due to their deterministic and superior space-filling nature. Two strategies to solve the inverse-source problem are proposed and were implemented in the stochastic stage. The original and scrambled versions of the Halton point-set and the original version of the Sobol sequence were found to produce the best results across all the test cases considered. Newton's method with the Tikhonov stabilizer and adaptive regularization with quadratic line-search was implemented in the gradient stage. The final solution obtained from the Newton's scheme is close to the true model parameters from the Copenhagen data. Future work will investigate and document the correlation between the star-discrepancy of a point-set and its effectiveness in the sampling procedure.

References

[1] Akecelik V, Biros G, Draganescu A, Ghattas O, Hill J and Waanders B V B 2006 Inversion of airborne contaminants in a regional model *Lecture Notes in Computer Science* **3993** pp 481-488

[2] Allen C T, Haupt S E and Young G S Application of genetic algorithm-coupled receptor/dispersion model to the dipole pride 26 experiments *14th Joint Conf. on the Applications of Air Pollution Meteorology with the Air and Waste Management*

[3] Allen C T, Young G S and Haupt S E 2007 Improving pollutant source characterization by better estimating wind direction with a genetic algorithm *Atmospheric Environment* **41** 2283-2289

[4] Anonymous 2004 Synopsis of the January 22-23, 2004 secretary's council on public health preparedness *Biosecurity and bioterrorism: biodefense strategy, practice, and science* **2(1)** pp 41-45

[5] Annunzio A J, Haupt S E and Young G S Source characterization and meteorology retrieval including atmospheric boundary layer depth using genetic algorithm *10th Conf. on Atmospheric Chemistry*

[6] Aster R.C, Borchers B and Thurber C *Parameter estimation and inverse problems* (Elsevier)

[7] Ballester P J and Carter J N 2006 Characterizing the parameter space of a highly nonlinear inverse problem *Inverse Problems in Science and Engineering* **14** 171-191

[8] Beck J V and Woodbury K A 1998 Inverse problems and parameter estimation: integration of measurement and analysis *Meas. Sci. Technol.* **9** 839-847

[9] Beychok M R *Fundamentals of stack gas dispersion* ISBN 0-9644588-0-2

[10] Bocquet M 2005 Reconstruction of an atmospheric tracer source using the principle of maximum entropy. I: Theory *Q. J. R. Meteorol Soc.* **131** 2191-2208

[11] Bradley M N, Kosovic B and Nasstrom J S 2005 Models and measurements: Complementary tools for predicting atmospheric dispersion and assessing the consequences of nuclear and

[4]Corresponding author: Bhagirath Addepalli, Department of Mechanical Engineering, MEB 2110, University of Utah, Salt Lake City, UT - 84112, U.S.A.

radiological emergencies *Int. Conf. on Monitoring, Assessments, and Uncertainties for Nuclear and Radiological Emergency Response*
[12] Brown M J, Williams M D, Streit G E, Nelson M and Linger S 2006 An operational event reconstruction tool: Source inversion for biological agent detectors *86th American Meteorological Society Annual Meeting*
[13] Chow F, Kosovic B and Chan S T 2006 Source inversion for contaminant plume dispersion in urban environments using building-resolving simulations *86th American Meteorological Society Annual Meeting*
[14] Davoine X and Bocquet M 2007 Inverse modelling-based reconstruction of the Chernobyl source term available for long-range transport *Atmos. Chem. Phys. Discuss* **7** 1-43
[15] Edwards D Practical sampling for ray-based rendering *A Thesis Submitted to the Faculty of The University of Utah in Partial Fulfilment of the Requirements for the Degree of Doctor of Philosophy, School of Computing*
[16] Frandsen P E, Jonasson K, Nielsen H B and Tingleff O *Unconstrained Optimization* Informatics and Mathematical Modelling Technical University of Denmark
[17] Gryning S E and Lyck E 1998 The Copenhagen tracer experiments: Reporting measurements. *Riso National Laboratory Roskilde*
[18] Hanson K M 2003 Quasi-Monte Carlo: Halftoning in high dimensions? *Proc. SPIE* **5016** pp 161-172
[19] Haupt S E, Haupt R L and Young GS 2007 Using genetic algorithms in chem-bio defense applications *Proc. of the 2007 ECSIS Symposium on Bio-inspired, Learning, and Intelligent Systems for Security* pp 151-154
[20] Haupt S E and Young GS 2008 Paradigms for source characterization *88th American Meteorological Society Annual Meeting*
[21] Hogan W R, Cooper G F, Wagner M M and Wallstrom G L An inversion Gaussian plume model for estimating the location and amount of release of airborne agents from downwind atmospheric concentrations *The RODS laboratory, University of Pittsburgh*
[22] Houweling S, Kamsinki T, Dentener F, Lelieveld J, Heimann M 1999 Inverse modelling of methane sources and sinks using the adjoint of a global transport model *Journal of Geophysical Research* **104** 137-26
[23] Islam M A 1999 Application of the Gaussian plume model to determine the location of an unknown emission source *Water, Air and Soil Pollution* **112** 241-245
[24] Kelley C T *Solving Nonlinear Equations with Newton's Method - Fundamentals of Algorithms* (SIAM)
[25] Kennett B L N 2004 Consistency regions in non-linear inversion *Geophys. J. Int.* **157** 583-588
[26] Khemka A, Bouman C A and Bell M R 2006 Inverse problems in atmospheric dispersion with randomly scattered sensors *Digital Signal Processing* **16** 638-651
[27] Lemieux C *Monte Carlo and Quasi-Monte Carlo Sampling* (Springer)
[28] Lomax A and Sneider R 1995 Identifying sets of acceptable solutions to non-linear, geophysical inverse problems which have complicated misfit functions *Nonlinear Processes in Geophysics* **2** 222-227
[29] Long K J, Haupt S E, Young G S and Allen C.T 2006 Characterizing contaminant source and meteorological forcing using data assimilation with a genetic algorithm *86th American Meteorological Society Annual Meeting*
[30] Matousek J 1998 On the L2-discrepancy for anchored boxes *Journal of Complexity* **14** 527–556
[31] Mosegaard K and Trantola A 1995 Monte Carlo sampling of solutions to inverse problems *Journal of Geophysics Research* **100** 431-12
[32] Niederreiter, H Random number generation and Quasi-Monte Carlo methods *CBMS-NSF Regional Conference Series in Applied Mathematics*
[33] Scales J A and Tenorio L 2001 Prior information and uncertainty in inverse problems *Geophysics* **66** 389-397

[4]Corresponding author: Bhagirath Addepalli, Department of Mechanical Engineering, MEB 2110, University of Utah, Salt Lake City, UT - 84112, U.S.A.

[34] Sambridge M, Beghein C, Simons F J and Sneider, R 2006 How do we understand and visualize uncertainty? *The Leading Edge* 542-546
[35] Sambridge M Inverse problems in a nutshell *Center for Advanced Data Inference, Research School of Earth Sciences, Australian National University ACT 0200 Australia*
[36] Senocak I, Hengartner N W, Short M B and Daniel B W 2008 Stochastic event reconstruction of atmospheric contaminant dispersion using Bayesian inference *Atmospheric Environment* **42** 7718-7727
[37] Sneider R 1998 The role of nonlineaity in inverse problems *Inverse Problems* **14** 387-404
[38] Sambridge M and Mosegaard K 2002 Monte Carlo methods in geophysical inverse problems *Reviews of Geophysics* **40** 1-29
[39] Sambridge M 2001 Finding acceptable solutions in nonlinear inverse problems using a neighbourhood algorithm *Inverse Problems* **17** 387-403
[40] Storch R B Pimentel L C G and Orlande H R B 2007 Identification of atmospheric boundary layer parameters by inverse problem *Atmospheric Environment* **41** 1417-1425
[41] Thomson L C, Hirst B, Gibson G, Gillespie S, Jonathan P, Skeldon K D and Padgett M J 2007 An improved algorithm for locating a gas source using inverse methods *Atmospheric Environment* **41** 1128-1134
[42] Trantola A *Inverse Problem Theory and Methods for Model Parameter Estimation* (SIAM)
[43] Turner B D *Workbook of Atmospheric Dispersion Estimates – An Introduction to Dispersion Modelling* (Lewis Publishers)
[44] Vogel C R Computational methods for inverse problems *Frontiers in Applied Mathematics* (SIAM)
[45] Wirgin A The inverse crime **LMA/CNRS, 31 chemin Joseph Aiguier, 13402 Marseille cedex 20, France*
[46] Zajic D and Brown M J 2008 Source inversion in cities using the collector footprint methodology *88th American Meteorological Society Annual Meeting*
[47] Zbinsky Z B *Stochastic Adaptive Search for Global Optimization* (Kluwer Academinc Publishers)
[48] Zhdanov M S *Geophysical Inverse Theory and Regularization Problems - Methods in Geochemistry and Geophysics* **36** (Elsevier)

[4]Corresponding author: Bhagirath Addepalli, Department of Mechanical Engineering, MEB 2110, University of Utah, Salt Lake City, UT - 84112, U.S.A.

Authors	Model parameters (m)	Forward model (A)	Inversion technique	Validation procedure	Application	Max. grid size	# of runs	Performance
[1]	Strength (Q_s)	Steady laminar incompressible Navier-Stokes solver + ADE	Adjoint method	Synthetic data without noise	Contamination event in the Greater Los Angeles Basin (GLAB)	361× 121× 21		1) 917,301 concentration unknowns per time step 2) Total of 40 time steps 74×10^6 space-time variables
[5]	Location (x_s, y_s,z_s), Strength (Q_s), Wind speed (u_s) Wind direction (θ_s) Boundary layer depth (δ_s)	Gaussian puff	Genetic algorithm	Synthetic data without noise	Source characterization of atmospheric contaminant dispersion including the boundary layer depth			
[12]	Location (x_s, y_s), Strength (Q_s)	Gaussian plume model	Detector footprint methodology	Synthetic data with and without noise	Event reconstruction of atmospheric contaminant dispersion			
[13]	Location (x_s, y_s, ,z_s), Strength (Q_s)	FEM3MP – 3D incompressible Navier-Stokes finite element code	Bayesian inference + MCMC	1) Synthetic data with and without noise around a cube 2) Joint Urban 2003 IOP3	Event reconstruction in urban environments using building resolving simulations	132× 146× 30 for JU2003 – IOP3		1) 2560 forward runs 2) Total computation time of over 12 hours using 1024 2.4GHz Xeon processors –

[4]Corresponding author: Bhagirath Addepalli, Department of Mechanical Engineering, MEB 2110, University of Utah, Salt Lake City, UT - 84112, U.S.A.

								equivalent to 17 days on 32 processors
[14]	z_s – Effective source altitude t_s – Temporal release profile	Chemistry transport model (CTM) – POLAIR 3D	Adjoint method		Reconstruction of Chernobyl accident source term			
[19]	Location (x_s, y_s), Strength (Q_s), Wind speed (u_s) Wind direction (θ_s) Stability Class	Gaussian plume model	Genetic algorithm	Synthetic data without noise	Event reconstruction of atmospheric contaminant dispersion	32× 32	10	1) 2000 generations for the meteorological parameters 2) 10,000 generations for x_s, y_s, Q_s, θ_s & stability
[22]	$f_{j,m}$ – Integrated surface emission over region 'j' & month 'm' s_{OH} – Parameterization for chemical removal of methane with hydroxyl radical s_{stea} – Stratospheric methane loss c_0 – Global mean methane concentration	Global atmospheric chemistry transport model (CTM)	Adjoint method	National Oceanic and Atmospheric Administration (NOAA) / Climate Monitoring and Diagnostics Laboratory (CMDL) cooperative air sampling network	Study of global-scale sources and sinks of methane			
[26]	Location (x_s, y_s, ,z_s), Strength (Q_s)	Gaussian dispersion model	Expectation – Maximizatio n algorithm	Synthetic data without noise	Source characterization using randomly			

[4]Corresponding author: Bhagirath Addepalli, Department of Mechanical Engineering, MEB 2110, University of Utah, Salt Lake City, UT - 84112, U.S.A.

			(EM)		scattered sensors			
[29]	Location (x_s, y_s), Strength (Q_s), Wind direction (θ_s)	Gaussian puff	Genetic algorithm + simplex optimization (Nelder-Mead)	Synthetic data without noise – identical twin experiment		32× 32	10	1) # of chromosomes = 1200 2) Mutation Rate = 0.015 3) 100 GA iterations
[36]	Location (x_s, y_s, ,z_s), Strength (Q_s), Wind speed (u_s) Wind direction (θ_s)	Gaussian plume model	Bayesian inference + MCMC	Copenhagen tracer experiments	Stochastic event reconstruction of atmospheric contaminant dispersion			50,000 MCMC evaluations
[40]	Longitudinal diffusivity (K_{xx}), Friction velocity (u^*), Monin-Obukhov length (L), Surface roughness (z_0)	2D advection – diffusion equation (ADE)	Least squares minimization by Levenberg-Marquardt method	Copenhagen tracer experiments	Identification of atmospheric boundary layer parameters			
[41]	Location (x_s, y_s, ,z_s), Strength (Q_s)	Gaussian plume model	Simulated annealing (SA)	Simulated experimental data	Use of atmospheric ethane concentration to locate ground-level sources	16× 16		4×10^6 iterations

Table. 1: Salient features of the various inversion techniques used to solve atmospheric source characterization problems

[4]Corresponding author: Bhagirath Addepalli, Department of Mechanical Engineering, MEB 2110, University of Utah, Salt Lake City, UT - 84112, U.S.A.